

# *A physically-based model for low-temperature plasticity in BCC metals*

**Thomas E. Buchheit, Corbett C. Battaile,  
Christopher R. Weinberger, Elizabeth A. Holm**

Computational Materials Science and Engineering Department,  
Sandia National Laboratories, Albuquerque, NM 87185-1411 U.S.A.

Sandia National Laboratories is a multi-program laboratory managed and operated by Sandia Corporation, a wholly owned subsidiary of Lockheed Martin Corporation, for the U.S. Department of Energy's National Nuclear Security Administration under contract DE-AC04-94AL85000.



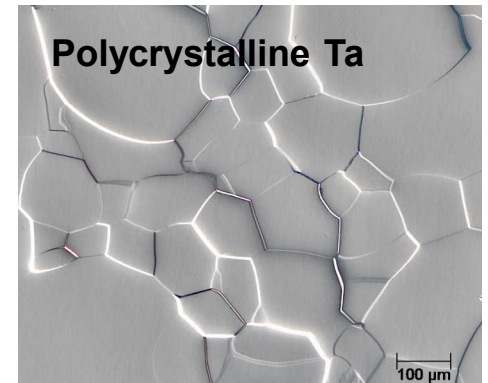
# Motivation for developing low-temperature BCC deformation models

---

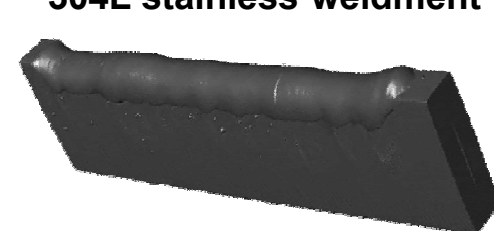
- BCC metals are scientifically interesting.
  - Technologically important.
    - *Refractories: W, Mo, Ta*
    - *Steel*
  - Underrepresented in computational materials science studies.
    - *Complex response, compared to FCC*
    - *Most models are phenomenological*
  - Favorable properties for experimental studies.
    - *Can prepare microstructures ranging from single crystal to nanocrystalline.*
    - *Favorable properties for microscopy and EBSD analysis.*



Single-crystal Ta

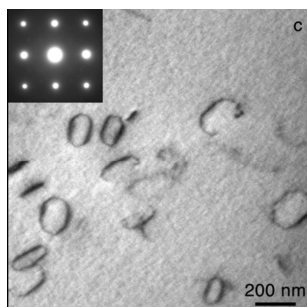
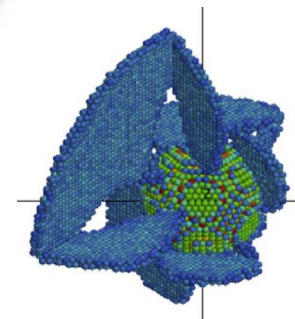


Polycrystalline Ta



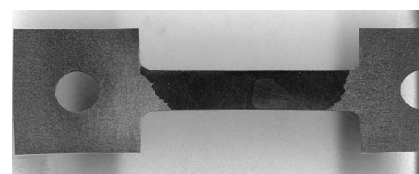
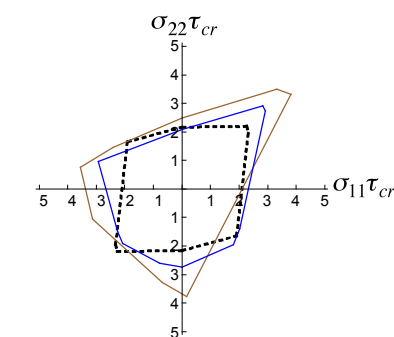
304L stainless weldment

# *Including microstructure in design and analysis*



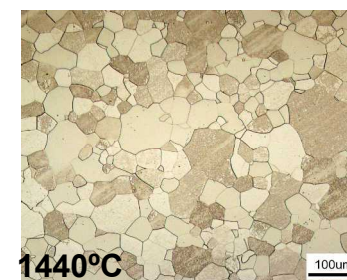
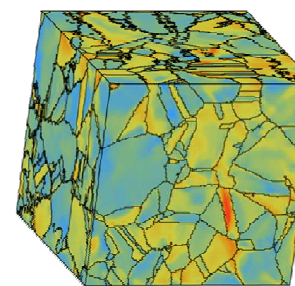
Atomic scale  
phenomena

$10^{-9}$  m  
 $10^{-9}$  s



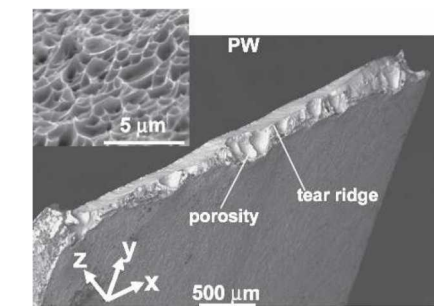
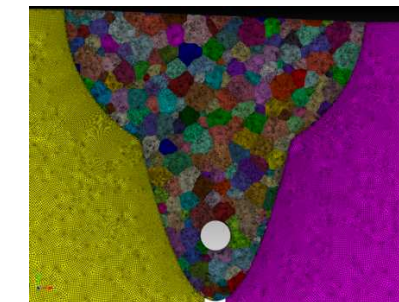
Single crystal  
behavior

$10^{-6}$  m  
 $10^0$  s



Microstructural  
effects

$10^{-3}$  m  
 $10^3$  s



Material  
performance

$10^0$  m  
 $10^6$  s



# How BCC and FCC crystal plasticity differ

- In BCC metals at low temperatures, slip occurs via the motion of screw dislocations along  $\langle 111 \rangle$  directions on  $(110)$  planes.

The plastic strain rate is given by:

$$D = \sum_s \dot{\gamma}^{(s)} \mathbf{m}^{(s)}$$

Schmid factor

$$\dot{\gamma}^{(s)} = G \left( \frac{\mathbf{m}^{(s)} : \boldsymbol{\sigma}}{\tau^{(s)}} \right)$$

**Note:**

FCC slip system:  $\langle 110 \rangle \{111\}$

BCC slip system:  $\langle 111 \rangle \{110\}$

$\therefore \mathbf{m}$  is the same for BCC and FCC

The lattice resistance on slip system  $s$  is:

$$\tau^{(s)} = \tau(T, \sigma) = \tau_{\text{obs}} + \tau_{\text{fric}}(T, \sigma) \rightarrow \text{Peierls stress}$$

$\tau_{\text{obs}}$   $\rightarrow$  Obstacle stress

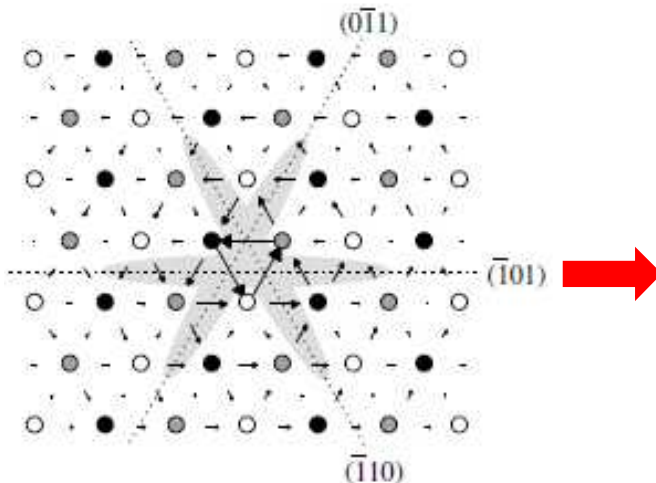
In FCC metals,  $\tau_{\text{obs}} \gg \tau_{\text{fric}}$   $\tau_{\text{fric}} \approx 0$

In BCC metals,  $\tau_{\text{fric}} \gg \tau_{\text{obs}}$   $\tau_{\text{obs}} \approx 0$

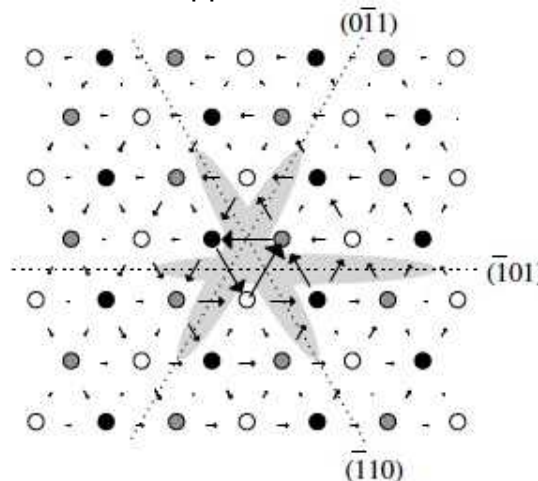
# Atomic Scale: Physical model for dislocation motion in BCC metals

- Atomic scale simulations show dislocation core spreading onto adjacent (110) planes in BCC metals.
  - Core spreading creates a significant Peierls barrier to dislocation motion.
  - Because the dislocation spreads onto three planes, motion can be affected by stress components outside the preferred slip plane, i.e. non-Schmid stresses.

[111] zone depiction of a relaxed screw dislocation core in Mo



Distortion of the dislocation core under an applied shear stress



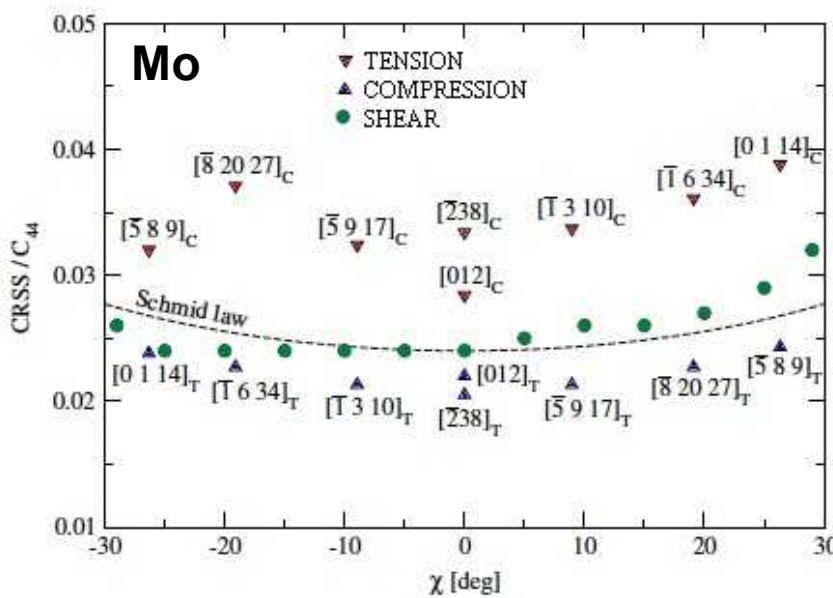
Groger, Vitek et al. *Acta Mat.* **56** (2008) 5412

# Implications of non-Schmid deformation

- The non-Schmid stress components arise from two causes:
  - Asymmetry within the slip plane (twinning/anti-twinning) is a minor effect.
  - Contributions by stress components outside the slip plane are significant.

*“...glide of the 1/2[111] screw dislocation [on the (-101) plane] depends on shear stresses both parallel and perpendicular to the Burgers vector that act not only in the slip plane but also in other {110} planes of the [111] zone.”*

-Groger, Vitek et al. *Acta Mat.* **56** (2008) 5412.



**The non-Schmid stress components cause the widely observed tension-compression asymmetry in BCC metals**

# Single crystal behavior: BCC crystal plasticity model

The atomic results can be fit to a yield criterion given by:

$$\sigma_{cr}^{app} \left[ a_0 \mathbf{m}^{(s)} \mathbf{n}^{(s)} + a_1 \mathbf{m}^{(s)} \mathbf{n}^{(s')} + a_2 \left( \mathbf{n}^{(s)} \times \mathbf{m}^{(s)} \right) \mathbf{n}^{(s)} + a_3 \left( \mathbf{n}^{(s)} \times \mathbf{m}^{(s)} \right) \mathbf{n}^{(s')} \right] = \tau_{cr}$$

↓
↓
↓

applied stress
stress projection tensor,  $\mathbf{P}_\sigma^{(s)}$ 
yield stress

We use this form to derive the generalized stress state on a slip system:

$$\tau^{(s)} = \mathbf{P}_\sigma^{(s)} : \boldsymbol{\sigma}^{app}$$

Which leads to a single-crystal constitutive law:

$$\dot{\gamma}^{(s)} = \frac{\tau^{(s)}}{\tau_{cr}} \left| \frac{\tau^{(s)}}{\tau_{cr}} \right|^{\frac{1}{m}-1}$$

Which gives the plastic strain rate:

$$\mathbf{D} = \sum \dot{\gamma}^{(s)} \mathbf{m}^{(s)}$$

# Material-specific constitutive parameters

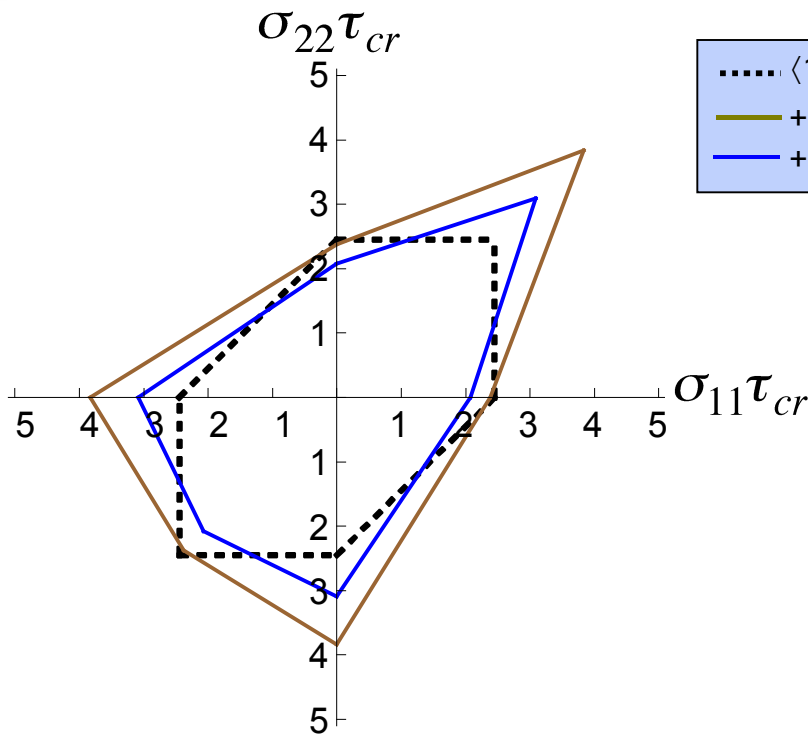
- The parameters  $a_0$ ,  $a_1$ ,  $a_2$  and  $a_3$  are determined from bond order potential atomistic simulations.

Parameter	FCC	W	Mo	
$a_0$	1	1	1	Schmid stress
$a_1$	0	0	0.24	twinning/anti-twinning
$a_2$	0	0.56	0	out-of-plane effects
$a_3$	0	0.75	0.35	out-of-plane effects
$\tau_{cr}$	1	1.36	1.26	

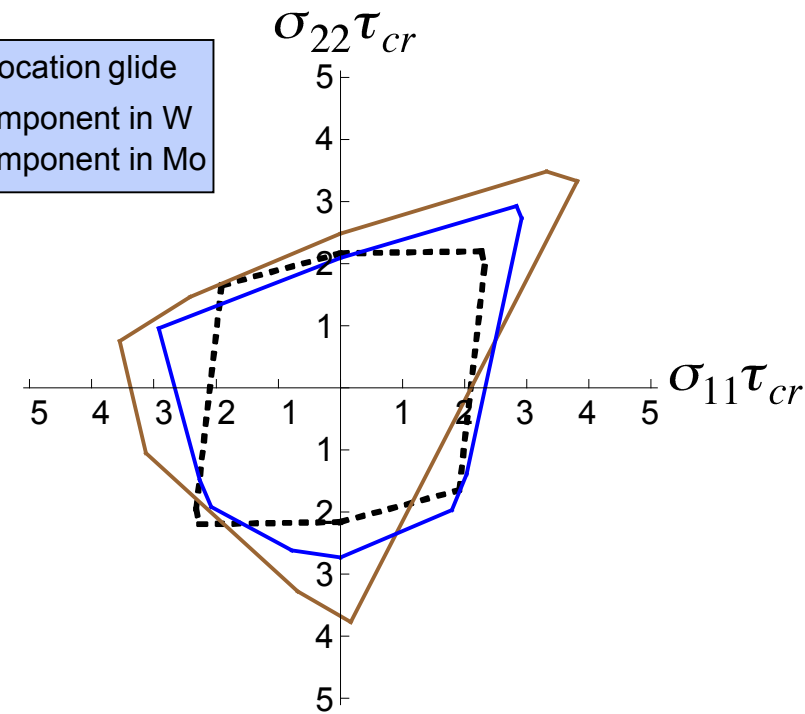
- Parameters are normalized such that  $\tau_{CRSS} = 1$ .

**Gap: To develop similar models for other BCC metals, such as Ta and Fe, we need valid interatomic potential functions.**

# Single Crystal Results: BCC single crystal yield surfaces



$\langle 100 \rangle(010)$  orientation  
highly symmetric

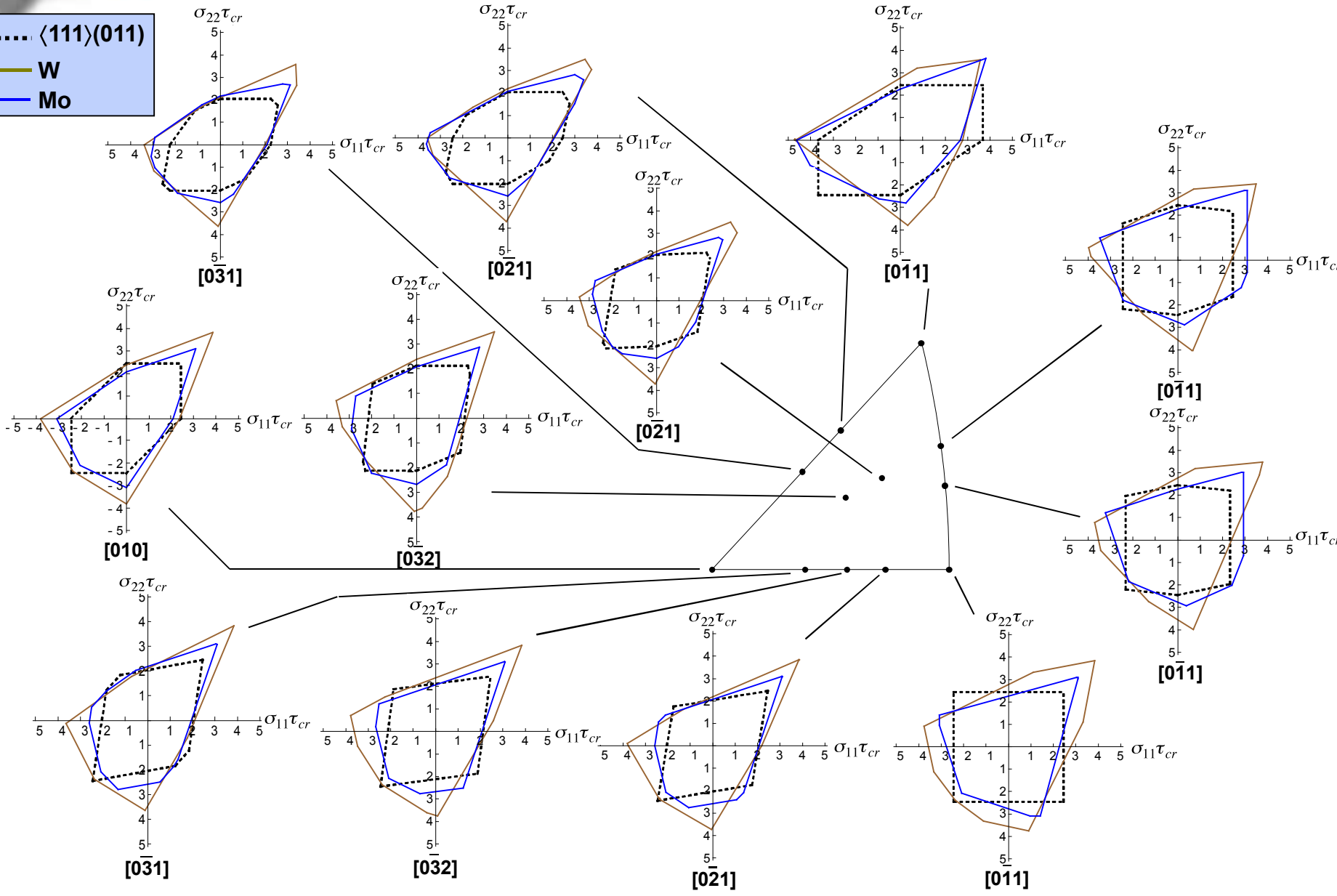


$\langle -0.180, 0.575, 0.798 \rangle, (0, -0.811, 0.585)$  orientation  
asymmetric

- BCC yield surfaces are considerably different from FCC yield surfaces.
- The yield surfaces of W and Mo are quite distinct.
- Tension/compression asymmetry is apparent.

# There is significant biaxial tension-compression asymmetry in BCC yield surfaces

-----  $\langle 111 \rangle \langle 011 \rangle$   
— W  
— Mo

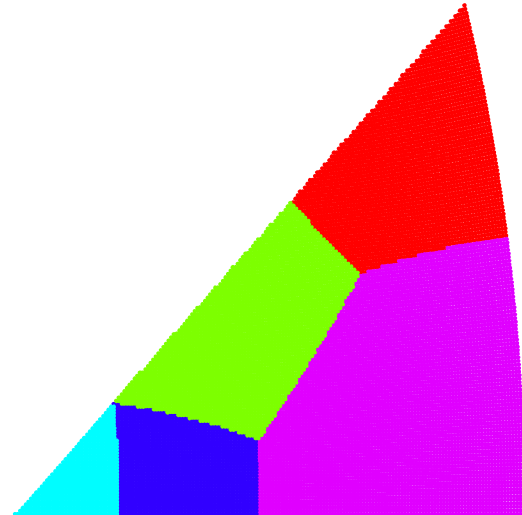
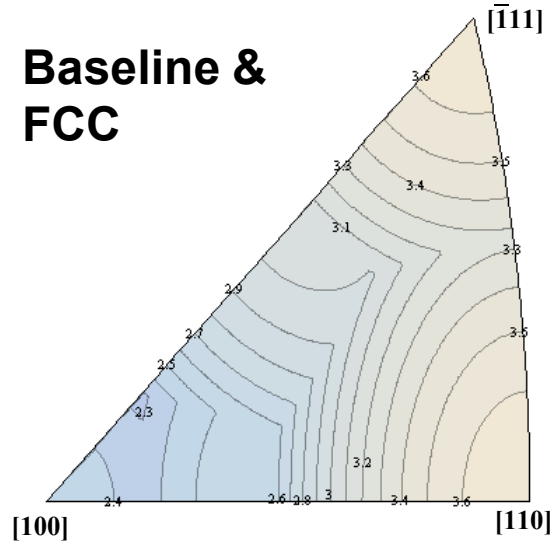




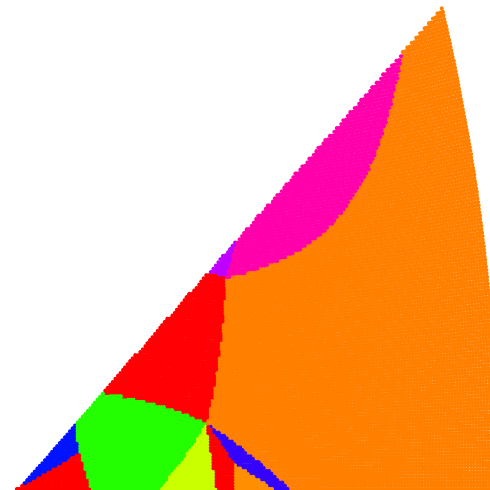
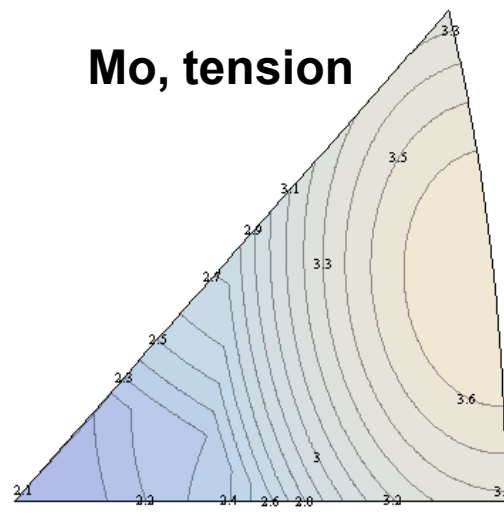
# Non-Schmid stresses significantly alter the Taylor factor landscape in BCC metals

---

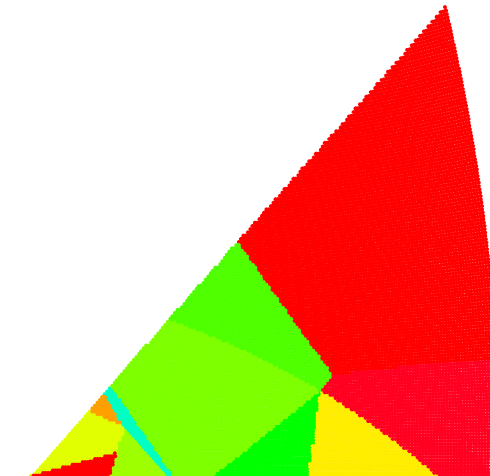
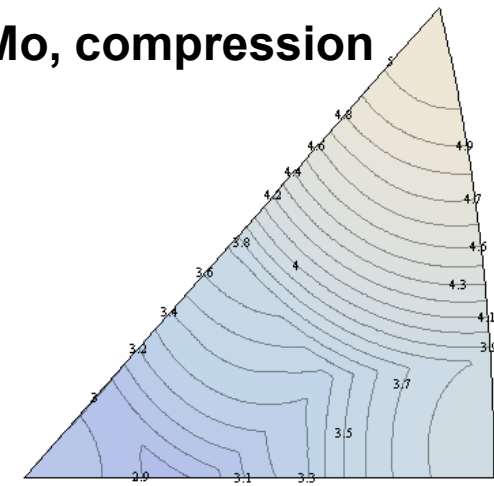
Baseline &  
FCC



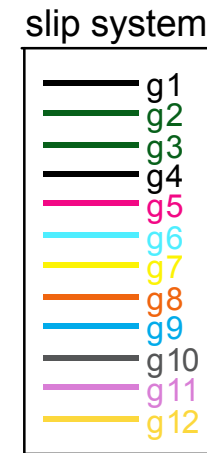
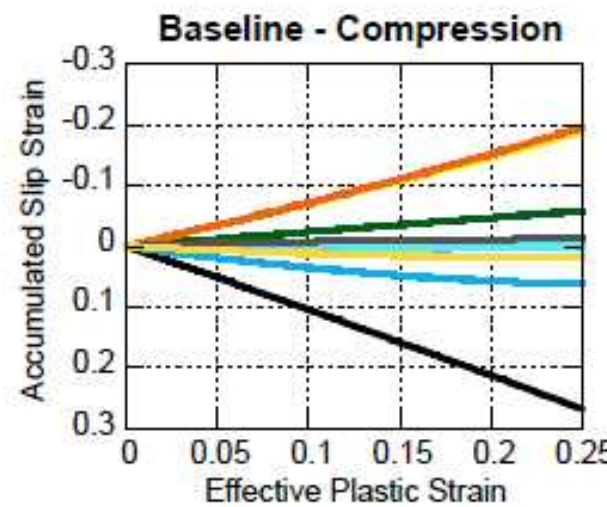
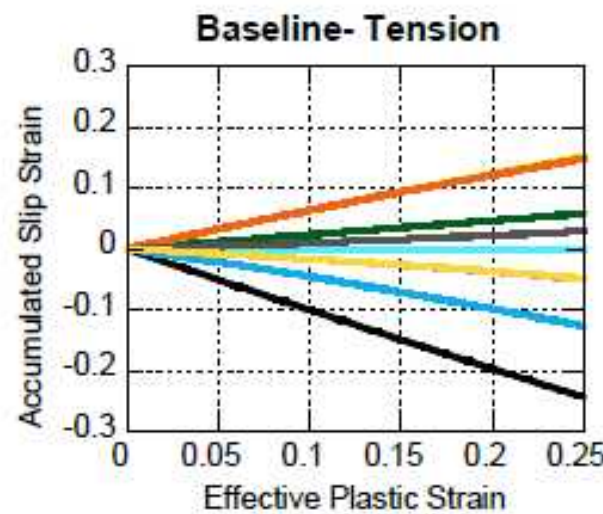
Mo, tension



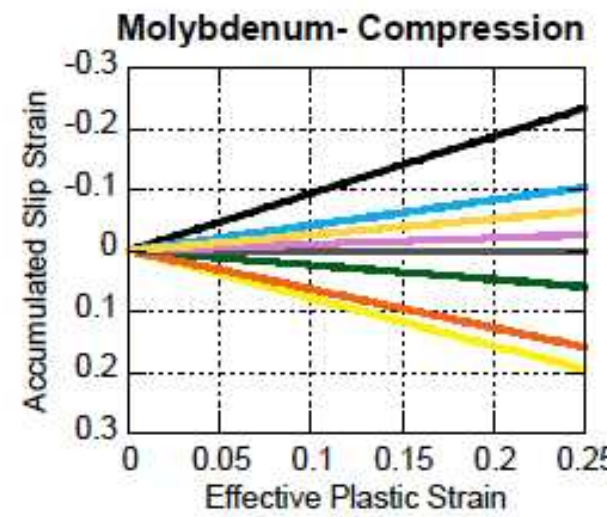
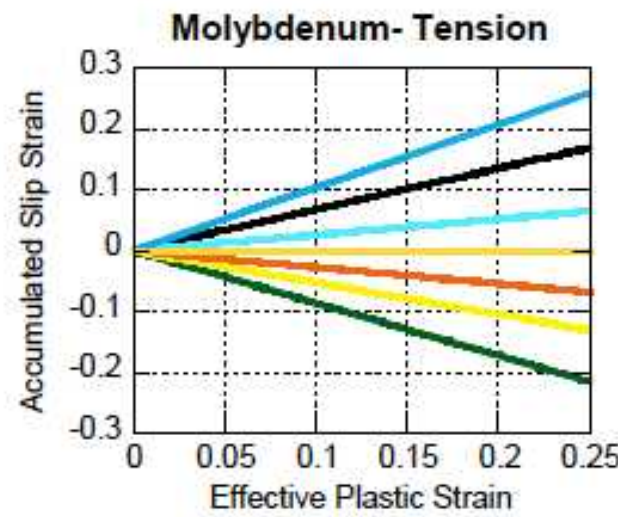
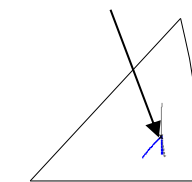
Mo, compression



# Non-Schmid stresses significantly alter slip system activity in BCC metals



crystal orientation:  
[-.180, 0.575, 0.798]



- Baseline is the same in tension and compression.
- Mo differs in tension and compression.
- Mo differs from baseline in tension and compression.



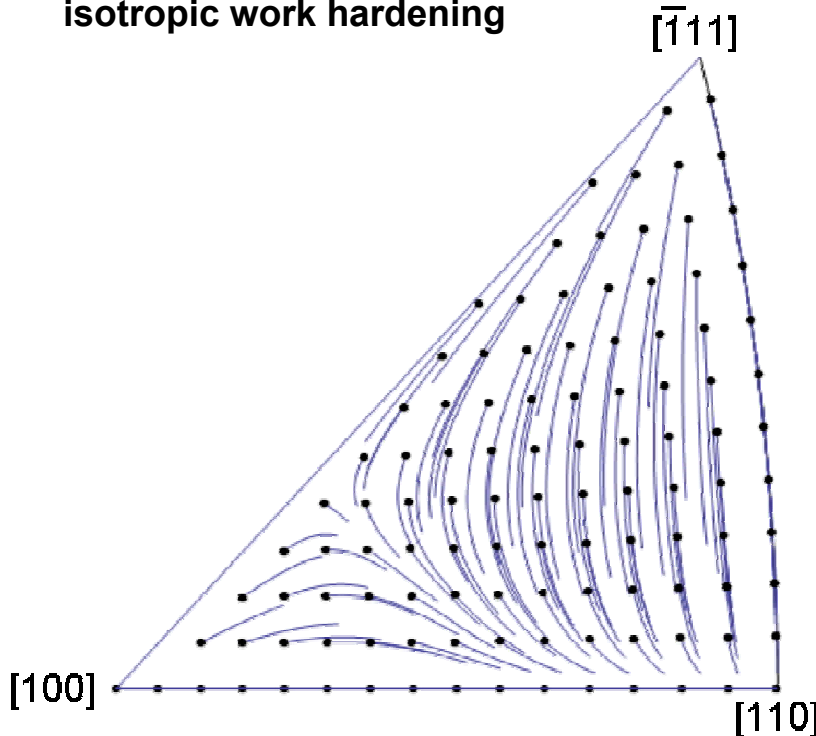
Sandia  
National  
Laboratories

# Non-Schmid stresses significantly alter crystal rotations in BCC metals

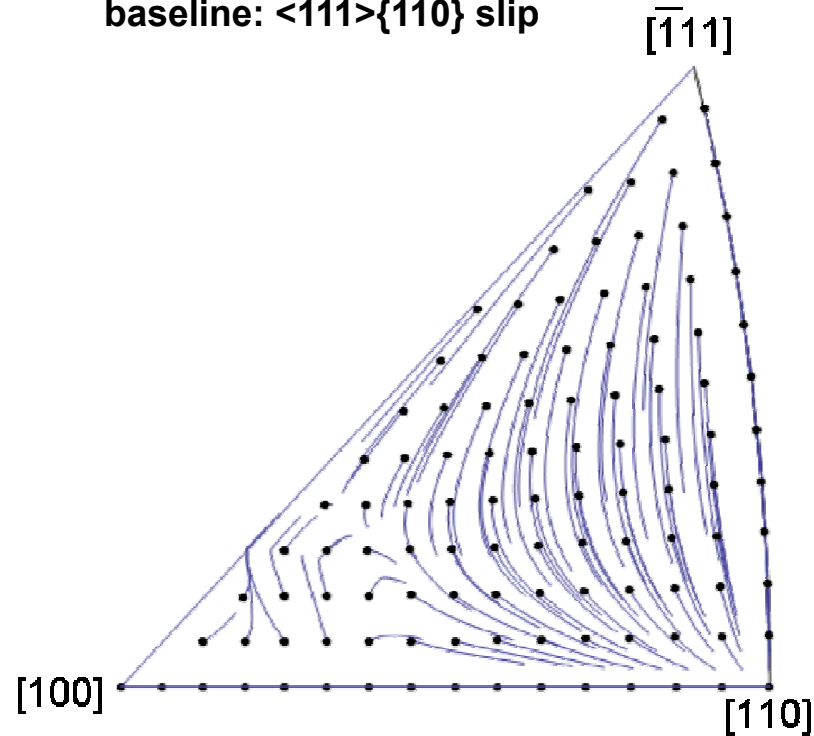
Isochoric Deformation to 50% strain:

$$\dot{\varepsilon} = \begin{pmatrix} 1 & 0 & 0 \\ 0 & -1/2 & 0 \\ 0 & 0 & -1/2 \end{pmatrix} dt$$

FCC crystal plasticity model with isotropic work hardening



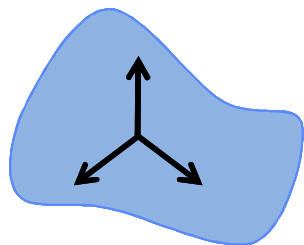
BCC crystal plasticity baseline: <111>{110} slip



# Extending single crystal behavior to capture microstructural effects

- Polycrystal plasticity models reveal how individual grains take part in polycrystalline deformation

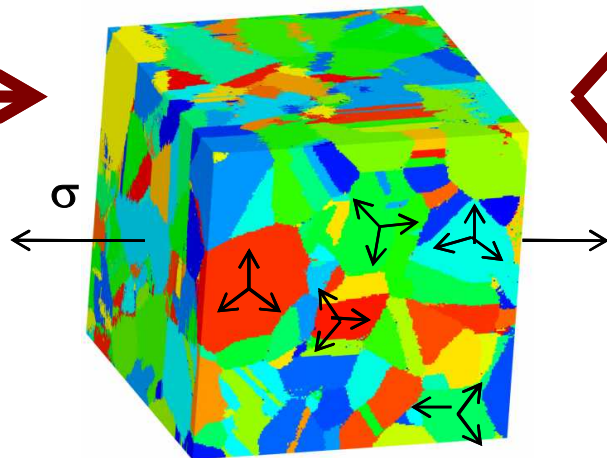
## Single crystal plasticity



Constitutive law

$$\dot{\gamma}^{(s)} = \frac{\tau^{(s)}}{\tau_{cr}} \left| \frac{\tau^{(s)}}{\tau_{cr}} \right|^{m-1}$$

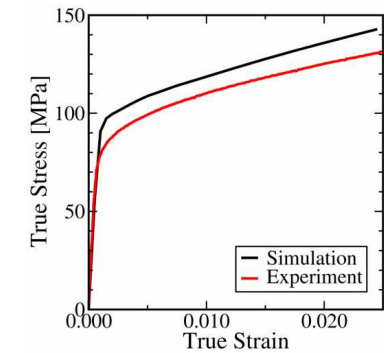
## Polycrystal plasticity



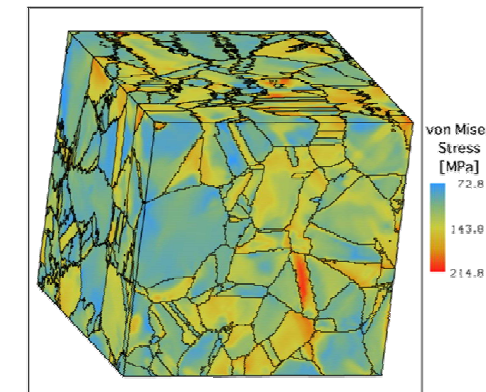
Each grain responds via the orientation-dependent constitutive law

## Results

Overall mechanical response

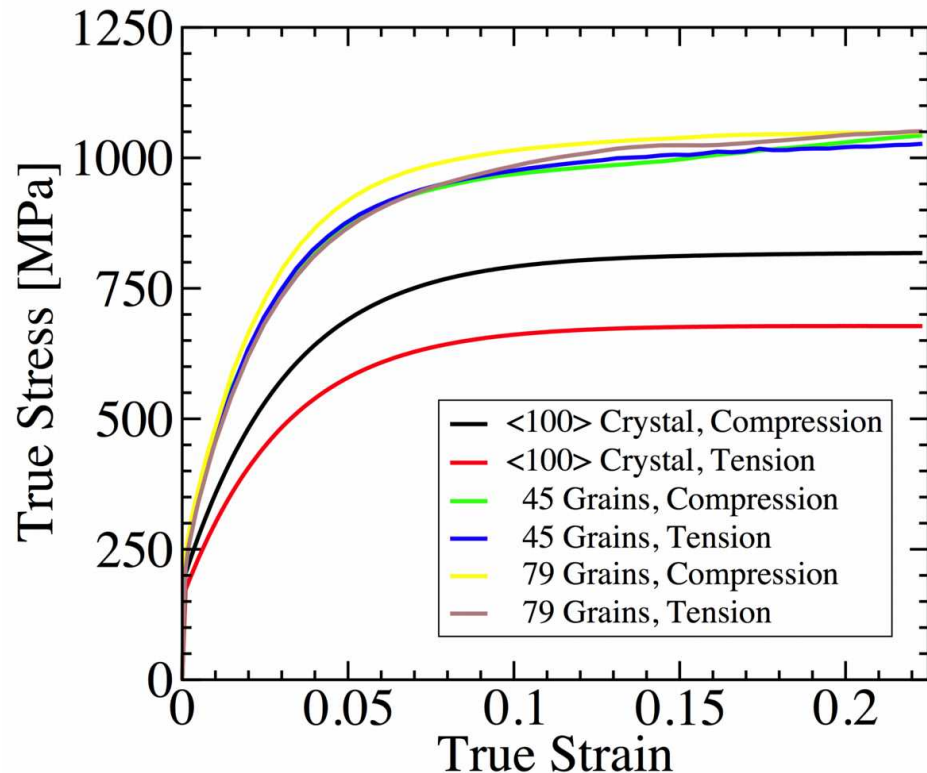


Individual grain response  
(rotation, stress, etc.)



# Microstructural Results: Continuum response of BCC polycrystals

- In plasticity simulations of single- and polycrystalline Mo:
  - *Single crystal and polycrystal response differ considerably.*
  - *Single crystals show considerable tension/compression asymmetry.*
  - *Polycrystals do not exhibit tension/compression asymmetry.*
  - *There is no grain size dependence in this model.*



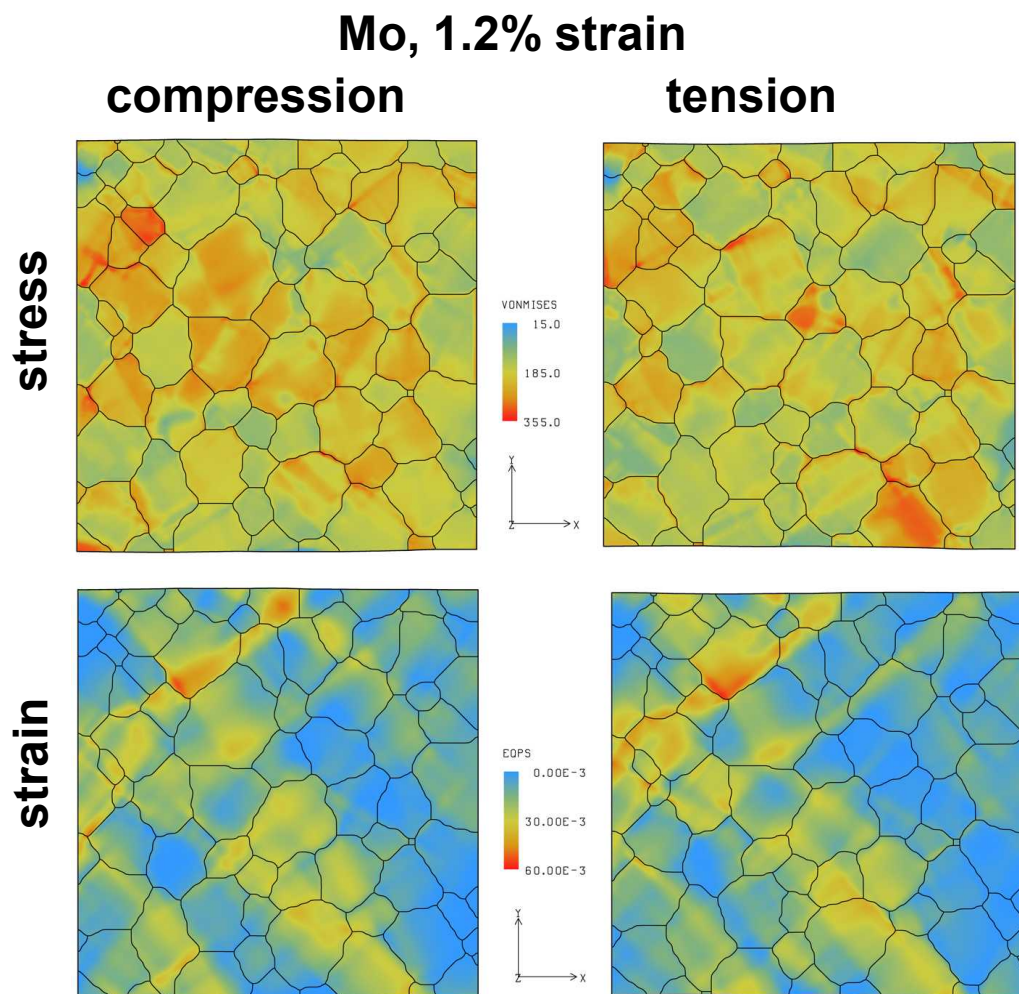


# Microstructural Results: Grain scale stress and strain partitioning

- At the grain scale, tension/compression asymmetry affects local stress distribution.
- Grain structure influences the distribution of local strains, but tension/compression asymmetry does not.
- Local strains are partitioned to accommodate global deformation.

➤ Grain-scale stresses adjust to produce the required local strain.

**Polycrystal plasticity reveals the complex interdependence of local stress and strain in BCC metals.**





## Summary and Conclusions

---

- BCC plasticity differs fundamentally from FCC plasticity
- A physically-based model captures key elements of BCC plasticity
  - *Tension/compression asymmetry and yield surfaces*
  - *Differences in Taylor factor, slip system activity, crystal rotation*
- Polycrystal plasticity reveals how single-crystal properties interact in realistic grain structures
  - *Tension/compression asymmetry is maintained*
  - *Significant stress concentrations occur*



## *Supplementary Slides*

---

# Polycrystal plasticity model

Cauchy stress resolved on each slip system:

$$\tau = \sigma : (\mathbf{s} \otimes \mathbf{m})$$

Cauchy stress  
from FE solver

Slip rate on each system:

$$\dot{\gamma} = \dot{\gamma}_o \left| \frac{\tau}{\tau_{CRSS}} \right|^{\frac{1}{m}} \text{sign}(\tau)$$

Plastic velocity gradient:

$$\hat{\mathbf{L}}_p = \dot{\gamma} (\hat{\mathbf{s}} \otimes \hat{\mathbf{m}})$$

Plastic deformation gradient:  
(Cayley-Hamilton theorem<sup>1</sup>)

$$\dot{\mathbf{F}}_p = \hat{\mathbf{L}}_p \bullet \mathbf{F}_p \Rightarrow \begin{cases} \mathbf{F}_p = \exp(\hat{\mathbf{L}}_p \Delta t) \mathbf{F}_p \\ \exp(\hat{\mathbf{L}}_p \Delta t) = I + \frac{\sin \phi}{\phi} \hat{\mathbf{L}}_p \Delta t + \frac{1 - \cos \phi}{\phi^2} (\hat{\mathbf{L}}_p \bullet \hat{\mathbf{L}}_p) \Delta t^2 \\ \phi = \Delta t \sqrt{\frac{1}{2} (\hat{\mathbf{L}}_p : \hat{\mathbf{L}}_p)} \end{cases}$$

Elastic deformation gradient and strain:

$$\mathbf{F}_e = \mathbf{F} \bullet (\mathbf{F}_p)^{-1} \Rightarrow \hat{\mathbf{E}}_e = \frac{1}{2} [(\mathbf{F}_e)^T \bullet \mathbf{F}_e - \mathbf{I}]$$

2nd Piola-Kirchhoff stress (hyper-elasticity):

$$\hat{\sigma}_{PK2} = \mathbf{C} : \hat{\mathbf{E}}_e$$

Updated Cauchy stress:

$$\sigma = \frac{1}{J^{\mathbf{F}_e}} [\mathbf{F}_e \bullet \hat{\sigma}_{PK2} \bullet (\mathbf{F}_e)^T]$$

Cauchy stress  
to FE solver

Updated crystallographic orientation:

$$\mathbf{F}_e = \mathbf{U}_e \bullet \mathbf{R}_e \Rightarrow \mathbf{R}_{lattice} = \mathbf{R}_e \bullet \mathbf{R}_h$$

Effective plastic strain:

$$\bar{\varepsilon}_p = \sqrt{\frac{2}{3} \mathbf{E}_p : \mathbf{E}_p}$$

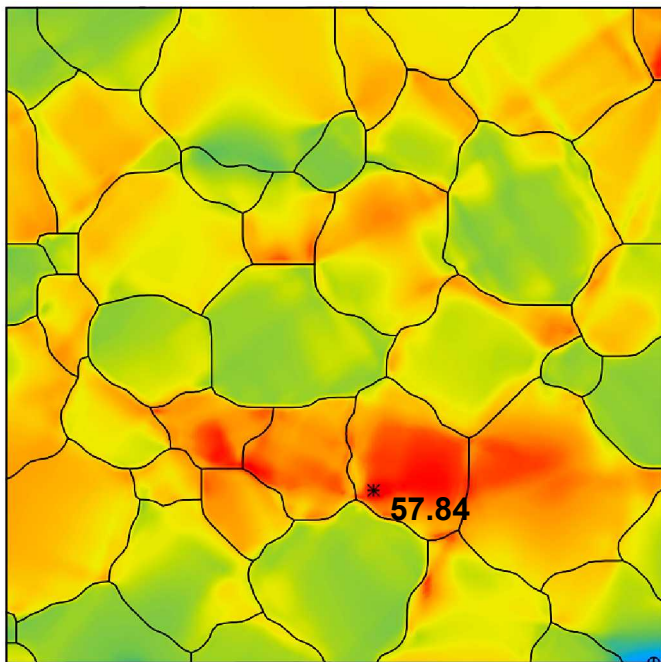
Updated “hardness” (CRSS):

$$\tau_{CRSS} = \tau_o + A \exp\left(-\frac{n}{A} \bar{\varepsilon}_p\right)$$

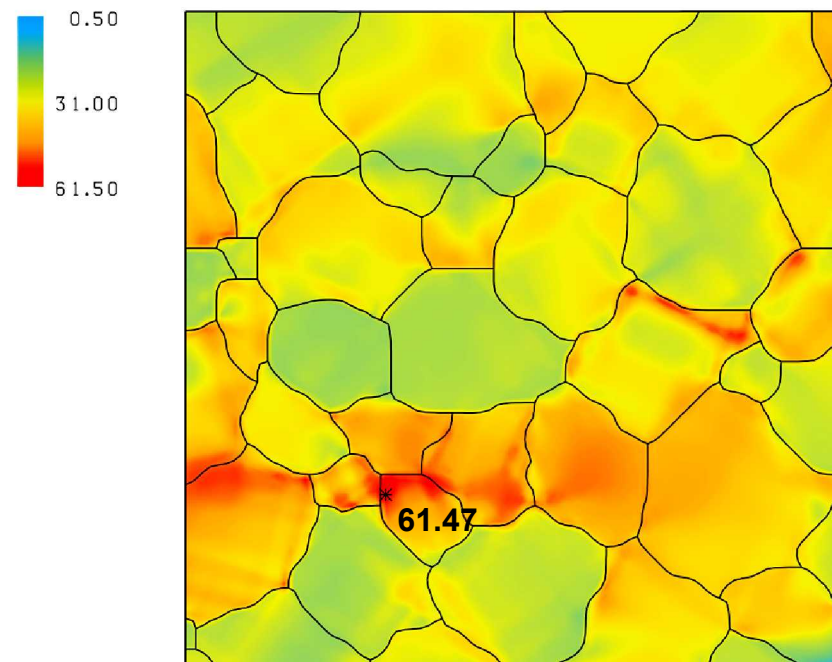
*Local stress concentrations are more severe prior to yielding*

---

**Von-Mises Stress Distribution in Mo (0.1% Strain)**



**Tension**



**Compression**